

1 **Flow behavior and thermal resistance of xanthan gum in formate**  
2 **brine**

3

4 Reinoso<sup>a</sup>, D.; Martín-Alfonso<sup>b</sup>, M.J.; Luckham<sup>c</sup>, P. F.; Martínez-Boza<sup>b\*</sup>, F.J

5 <sup>a</sup>International Institute for Nanocomposites Manufacturing (IINM), University of  
6 Warwick. (UK)

7 <sup>b</sup>Centro de Investigación en Tecnología de Procesos y Productos Químicos (Pro<sup>2</sup>Tec).  
8 Universidad de Huelva. (Spain)

9 <sup>c</sup>Department of Chemical Engineering. Imperial College London. (UK)

10

11 \*Corresponding author: [martinez@uhu.es](mailto:martinez@uhu.es)

12

13 ©2025. This manuscript version is made available under the CC-BY-NC-ND 4.0  
14 license <https://creativecommons.org/licenses/by-nc-nd/4.0/>

15

16 **Abstract**

17 Drilling and completion operations in HP/HT environments demand the use of  
18 environmentally friendly fluids with suitable properties such as solid-free high-density  
19 and pseudoplastic behavior. Xanthan gum solutions in different brines may be an  
20 interesting alternative to ensure a suitable thermo-rheological behavior and  
21 biodegradability. Nevertheless, xanthan exposed at high temperature experiences  
22 thermal degradation that can modify the flow properties over time and limits the ceiling  
23 temperature of oilfield applications. To gain insight on this issue, this paper  
24 characterizes the flow behavior of low concentration XT solutions in calcium and  
25 potassium brines, evaluating the effect that potassium formate exerts on both the flow  
26 properties and the resistance to thermal degradation of xanthan solutions as a function  
27 of the biopolymer concentration. Xanthan in formate brine retains the pseudoplastic  
28 behavior up to 190°C, however, low concentrate solutions undergo a thermal  
29 degradation that decreases the recovery of pseudoplasticity after being exposed to high  
30 temperature.

31       Keyword: xanthan gum, formate brine, flow behavior, thermal resistance

32

## 33        **1. Introduction**

34    Water soluble biopolymers are an interesting alternative in the oil industry to develop  
35    environmentally friendly fluids due to their biodegradability and harmless  
36    characteristics. Polysaccharide biopolymers are being used widely in the oilfield as  
37    viscosifiers for flooding and drilling operations due to their pseudoplastic behavior, at  
38    low concentrations and moderate temperatures, and their high resistance to shear  
39    degradation (Wei et al., 2014; Jang et al., 2015; Ghomrassi-Barr and Aliouche, 2016).  
40    New drilling and completion of deeper wells, horizontal drilling and slim-hole  
41    operations demand the use of environmentally friendly fluids with selected properties  
42    such as solid-free high-density and suitable viscosity versus shear rate (Boul et al.,  
43    2017). These fluids can be formulated using biopolymer solutions in monovalent and  
44    divalent cation brines. High solubility salts (i.e. formate, chloride and bromide brines)  
45    are preferable to achieve the required density to compensate the formation pressure.  
46    High molecular weight biopolymers (i.e xanthan, guar, wellan, etc.) are selected to  
47    ensure a suitable thermo-rheological behavior, to carry and maintain in suspension the  
48    drilled cuttings, to resist thermal degradation at the temperature of the well, and to  
49    guarantee the biodegradability of the post-operations waste fluids (Caenn et al., 2017).  
50    Among biopolymers, xanthan gum (XT) may be preferable due to both its excellent  
51    solubility in water and brines and its satisfactory rheological properties at low  
52    concentrations, compared to others biodegradable polymers such as guar gum, wellan  
53    gum and scleroglucan (Howard et al., 2015). These characteristics cover a wide range of  
54    engineering requirements, from high viscosity at low shear rate, necessary when the  
55    flow is stopped, to low viscosity at high shear rate for easy pumping circulation (Asafa  
56    and Shah, 2014; Hermoso et al., 2015).

57 The thermo-rheological properties of XT in water solutions have been described in the  
58 literature with the help of both linear oscillatory shear (Choppe et al., 2010; Rochefort  
59 and Middleman, 1987; Whitcomb and Macosko, 1978) and viscous flow techniques  
60 (Dario et al., 2011; Marcotte et al., 2001). These properties have been explained on the  
61 basis of time-dependent structures. The most accepted structure for XT in solution is a  
62 partially ordered broken helix that undergoes a progressive order-disorder transition. In  
63 the ordered state, XT solutions show the rheological behavior of a weakly structured  
64 material, characterized by a tendency to reach a high value of the Newtonian viscosity,  
65 in the low shear-rate region, and a pseudoplastic fall, characterized by an exponential  
66 decrease of the viscosity in the intermediate shear-rate region. In the disordered state,  
67 XT solutions lose their pseudoplasticity and behave as a low viscosity liquid (Choppe et  
68 al., 2010). Variables such as the chemical composition and concentration, side-chain  
69 substituents, presence of ions, pH, and temperature may influence the structure, and  
70 consequently, the rheological behavior of the solution and its engineering properties  
71 (Garcia-Ochoa et al., 2000; Sutherland, 1994).

72 The presence of salt heavily influences the order-disorder state of XT in solution and its  
73 engineering properties. At low concentration, the polymer chains contract by the  
74 screening effect of cations, decreasing the viscosity of the solution. For higher  
75 concentrations, the ordered conformation improves the gel-like behavior by associations  
76 with hydrogen bonds, altering the shear viscosity, depending on the saline strength and  
77 pyruvate content of the polymer (Fitzpatrick et al., 2013). When the temperature  
78 increases, the order-disorder conformational transition takes place, depending on  
79 concentration of both salt and polymer and the type of anions present in the solution, the  
80 rheology of the solution changes from gel-like behavior to the Newtonian flow (Wyatt  
81 and Liberatore, 2009).

82 The influence of salts on both the rheological and thermal properties of xanthan  
83 solutions is very important to design solid-free drilling and completion fluids. Suitable  
84 rheological behavior, preselected density and thermal resistance can be combined by  
85 controlling the type of salt and its concentration (Hermoso et al., 2017). In these  
86 solutions, salts can act not only as weighting agents for adjusting density but also as  
87 thermal stabilizers, extending the range of temperature where the solution retains its  
88 pseudoplastic behavior (Bradshaw et al., 2006). In this sense, formate salts improve  
89 significantly both the density and the resistance to thermal degradation of XT in brine  
90 solutions (Howard et al., 2015), being extensively used in many HP/HT challenged  
91 fields with success (Gao, 2019). Nevertheless, the formulations of formate drilling  
92 fluids with biopolymers such as XT have limited thermal resistance to degradation at  
93 high temperature, being a challenge to increase both the time of exposure at high  
94 temperature and the temperature ceiling for application in HP/HT environments.  
95 However, there are in the open literature few papers devoted to the study of the flow  
96 behavior of XT in formate brines at high temperatures and the influence of the thermal  
97 degradation on the pseudoplastic properties of these solutions.  
98 To bridge this knowledge gap, in a previous study (Reinoso et al., 2019) we discussed  
99 the rheological behavior of the solution of xanthan gum at 1 wt% in concentrate  
100 chloride and formate brines, concluding that potassium formate shifts the thermal  
101 transition of the biopolymer to higher temperatures, enlarging the range of temperature  
102 at which the solution behaves as a weak gel. In this paper, we focus on the study of the  
103 flow behavior of low concentration solutions in calcium and potassium brines,  
104 evaluating the effect that potassium formate exerts on both the flow properties and the  
105 resistance to thermal degradation of xanthan solutions as a function of the biopolymer  
106 concentration. Potassium formate brine enhances the resistance of xanthan solutions to

107 thermal degradation, improving the conservation of the pseudoplasticity proportionally  
108 to XT concentration and suggests that XT in potassium formate brines would extend the  
109 operational temperature range of any drilling fluid where it is present.

## 110 2. Materials and methods

111 Native XT solutions were prepared by adding xanthan powder ( $M_w \sim 10^6$  g/mol; lot  
112 0066563; Guinama S.L., Spain) without purification to distilled water, 0.01 wt%  
113 sodium azide (Sigma–Aldrich Co., Germany) was added to the solution as a  
114 preservative. The polymer was slowly added to water using a magnetic stirrer,  
115 maintaining the solution at rest to fully hydration for 24h, after which, the solutions  
116 were stirred in a Silverson mixer at 25°C, at 600 and 2000 rpm for 15 minutes  
117 respectively.

118 Brine solutions were prepared by dissolving potassium formate, potassium chloride or  
119 calcium chloride salts (all from Sigma–Aldrich Co., Germany), in the native XT  
120 solutions previously prepared until saturation, at room temperature ( $\sim 20^\circ\text{C}$ ), using a low  
121 shear mixer at 500 rpm (235 g KFo/100 ml; 34.4 g KCl/100 ml; 98.2  $\text{CaCl}_2 \cdot 2\text{H}_2\text{O}$ /100  
122 ml). The density of the XT saturated brine solutions was measured at 20°C with an  
123 Anton Paar DMA5000 densimeter, resulting  $1.5004 \pm 0.0005$  g/mL,  $1.1728 \pm 0.0002$  g/mL  
124 and  $1.4115 \pm 0.0003$  g/mL respectively.

125 The rheological characterization was carried out using a controlled stress rheometer  
126 Physica MCR-301 (Anton Paar, Austria), equipped with a pressure cell and coaxial  
127 cylinder geometries CC33/PR/XL and DG35.12/PR. A conventional coaxial cylinder  
128 CC28 was used as reference geometry at standard pressure.

129 Steady-state flow curves were conducted in the range of temperature of 20 to 190°C.  
130 Samples were loaded into the pressure cell at room temperature and pressurized with an  
131 inert gas ( $\text{N}_2$ ) to avoid vaporization of water at temperatures above 100°C. The pressure

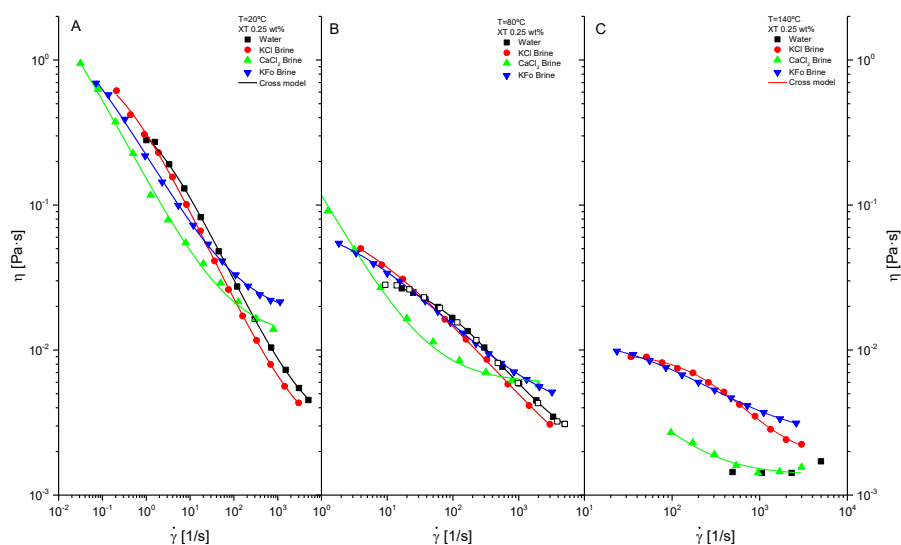
132 cell was heated to achieve the measuring temperature and the pressure was maintained  
133 at 50 bar throughout an automatic Isco pump model 260D (Isco Teledyne, USA). The  
134 flow curves were obtained by increasing the shear rate (upward curve) and then  
135 decreasing the shear rate, with the data collected over a period of 60 seconds at each  
136 shear rate, in the controlled shear rate mode of the rheometer. The effect of the  
137 pressurizing inert gas and thermal degradation were studied comparing flow curves at  
138 80°C. At least two replicates of each test were undertaken, with a standard deviation  
139 among replicates within  $\pm 5\%$ .

### 140 **3. Results and discussion**

141 Figure 1 shows the flow curves for low concentrate XT solutions (0.25 wt%) in  
142 potassium and calcium brines, at selected temperatures. As can be seen on Figure 1A, at  
143 20°C, both native and brine XT solutions behave as non-Newtonian shear-thinning  
144 fluids, showing a high degree of sensitivity to shear-rate, that can be measured by the  
145 slope of the viscosity versus shear rate. At this temperature, the XT solution at 0.25  
146 wt% would adopt a partial self-associated structure (Rochefort and Middleman, 1987;  
147 Ross-Murphy, 1995; Pelletier et al., 2001) that partially disrupts under shear, showing a  
148 shear-thinning behavior due to the orientation of the polymer chains in the direction of  
149 flow as the shear rate increases. This shear-thinning or pseudoplasticity can be  
150 quantified by means of characteristic parameters from different models such as the  
151 power law (Song et al., 2006), Hershel-Bulkley (Choppe et al., 2010), Carreau model  
152 (Jang et al., 2015) and Cross model (Fitzpatrick et al., 2013). For this study, several  
153 engineering parameters such as the limiting viscosity at both high shear-rate,  $\eta_{\infty}$ , and  
154 low shear-rate,  $\eta_0$ , the flow index  $m$  and the consistency index  $k$ , have been quantified  
155 with the help of the Cross' model (Cross, 1965):

156 
$$\eta = \eta_{\infty} + \frac{\eta_0 - \eta_{\infty}}{1 + (k \cdot \dot{\gamma})^m} \quad (1)$$

157 The presence of cations increases the pseudoplasticity of XT at 0.25 wt% in  
158 concentrated brines. The index  $m$  decreases in the order potassium chloride, calcium  
159 chloride and potassium formate brine, from 0.665 for native xanthan up to 0,554 for  
160 formate brine, at 20°C. In the low shear rate region, the native XT solution at 0.25 wt%,  
161 shows a tendency to reach the Newtonian plateau. The value of the zero-shear-limiting  
162 viscosity predicted by the Cross' model for the native XT solution is lower than that for  
163 the brine solutions as has been previously reported by Wyatt and Liberatore (2009) and  
164 Wyatt et al. (2011). Nevertheless, at intermediate shear rates, the viscosity of native XT  
165 solution is higher than those for brine solutions. The decrease of viscosity at low  
166 concentrations of XT in solution in the presence of salt has been attributed to the  
167 screening effect of charge that shrinks the polymer chains in the brine solutions,  
168 decreasing the interaction among them (Bergmann et al., 2008; Nieto et al., 2018). In  
169 the high shear rate region, XT in calcium chloride and potassium formate achieve higher  
170 values of the limiting viscosity than those for the native and the potassium chloride  
171 brine solutions, at low and intermediate temperature (Figure 1A and 1B). This fact  
172 indicates lower orientation of the entangled polymer chains in the direction of the flow  
173 for higher concentrated brines (due to the higher solubility in water of calcium chloride  
174 and potassium formate compared to potassium chloride brine). It is likely that, the  
175 polymer chains in high ionic strength solution develops robust entangled rod-like  
176 structures that increases the hydrodynamic volume under flow, increasing the values of  
177 the infinite-shear-limiting viscosity (Mezger, 2014).



178

179 **Figure 1. Evolution of the viscosity versus shear rate as a function of both temperature and type of brine for**  
 180 **xanthan gum 0.25wt%. A) 20°C. B) 80°C. C)140°C.**

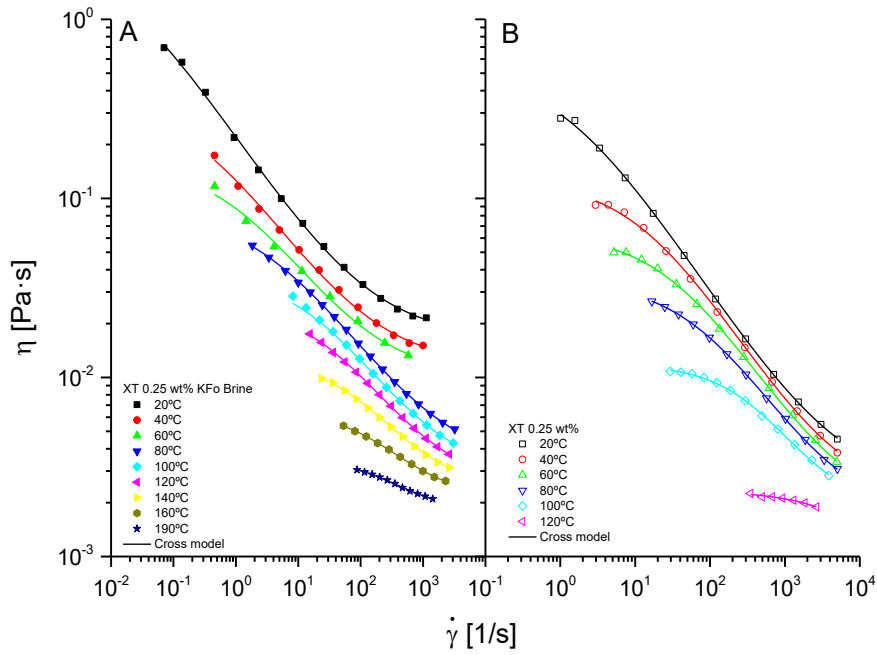
181

182 At 80°C, the degree of shear-thinning for both the native XT solution and potassium  
 183 brines decreases (values of the index  $m$  increase up to 0.755 for native XT and 0.705  
 184 and 0.630 for chloride and formate brines respectively), being nearly insensitive to  
 185 temperature for calcium brine (Figure 1B). At this temperature, the viscosity values for  
 186 XT in brine are higher than those for the native solution at low shear rates, being very  
 187 similar when the shear rate increases. Native XT solution progressively undergoes the  
 188 order/disorder transition from a partially ordered random broken helix to a disordered  
 189 random coil conformation at this temperature. XT solution becomes less viscous and  
 190 less sensitive to shear as have been previously reported by Pelletier et al. (2001). In  
 191 brine solutions, the self-association by hydrogen bonds, which may increase the shear-  
 192 thinning region and shifts the transition temperature to higher values, competes with the  
 193 shielding effect of divalent cations that may decrease the viscosity values. The former  
 194 phenomenon would be predominant in the case of potassium brines and the later in the  
 195 case of calcium brine. In the high shear rate region, the rod-like entangled chains hinder

196 the orientation into the flow direction, which could explain the increase in viscosity  
197 (Mezger, 2014). As can be seen in Figure 1B, the presence of the pressurizing gas (50  
198 bar of N<sub>2</sub>) does not influence significantly the flow behavior of xanthan solutions since  
199 both curves at atmospheric pressure and pressurized with 50 bar of N<sub>2</sub> were inside of the  
200 variability among replicates.

201 At higher temperatures, native XT solution behaves almost as a Newtonian liquid of  
202 low viscosity. Brine solutions shift the XT structural transition to higher temperatures,  
203 retaining the non-Newtonian properties over a large range of temperatures (Howard et  
204 al., 2015; Reinoso et al., 2019). As can be seen in Figure 1C, at 140°C, XT 0.25 wt% in  
205 potassium brines show shear-thinning behavior with indices  $m$  of 0.923 and 0.756 for  
206 chloride and formate brines respectively. XT in calcium brine shows significantly lower  
207 viscosity at the same shear rate and an index  $m$  near the unity (0.998). Nevertheless, the  
208 increase of the viscosity; at higher shear rate, for both the native and the calcium  
209 chloride solutions maybe artefact due to the contribution of the turbulent flow. The  
210 degradation of the viscous properties for XT solution of similar concentration in  
211 calcium brines has been previously reported by Xie and Lecourtier (1992) and it has  
212 been attributed to the thermal transition that the biopolymer undergoes at lower  
213 temperatures in calcium than in potassium brines (Seright and Henrici, 1990).

214 The properties of formate salts (mainly high solubility in water and the antioxidant  
215 properties of the formate anion) make these compounds better than other salts (chloride  
216 and bromide) for the formulation of solid-free drilling and completion fluids (Howard et  
217 al., 2015; Reinoso et al., 2019). Formate salts provide a large range of fluid density,  
218 while at the same time increase both the range of pseudoplastic behavior of the solution  
219 and its thermal resistance. In this sense the evolution of the flow properties of XT in  
220 concentrate formate brine as function of biopolymer concentration has been studied.

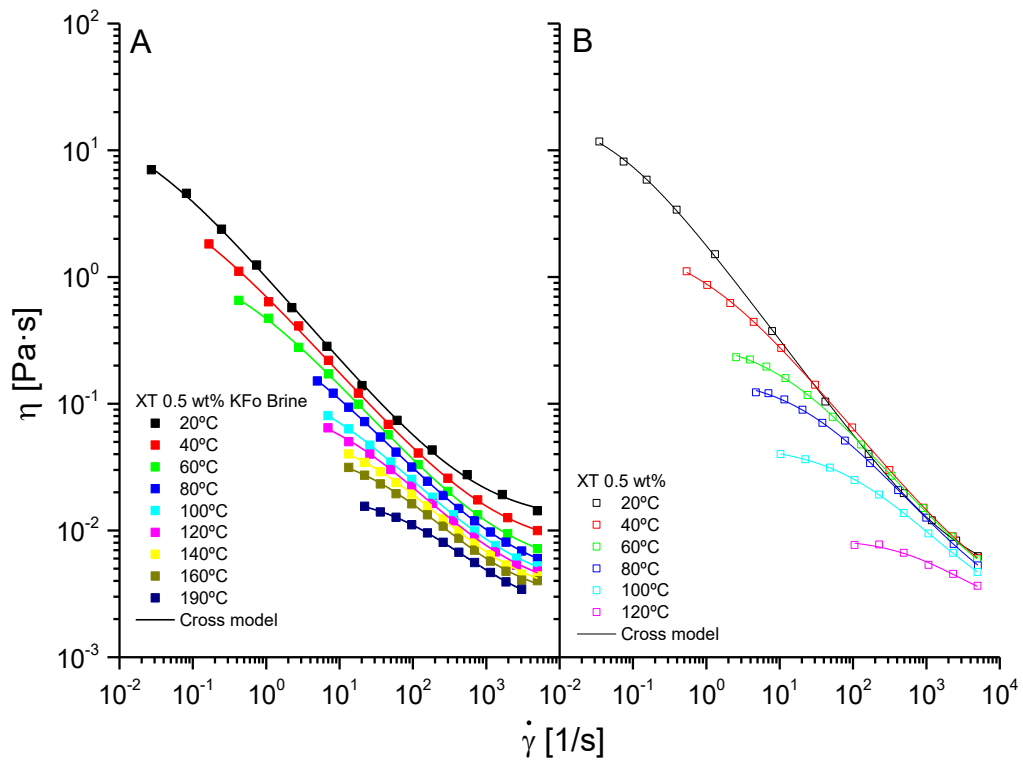


222

223 **Figure 2. Evolution of the viscosity versus shear rate as a function of the temperature. A) Xanthan gum**  
 224 **solution at 0.25wt% in potassium formate (KFo) brine. B) Xanthan gum solution at 0.25wt% in distilled water.**  
 225

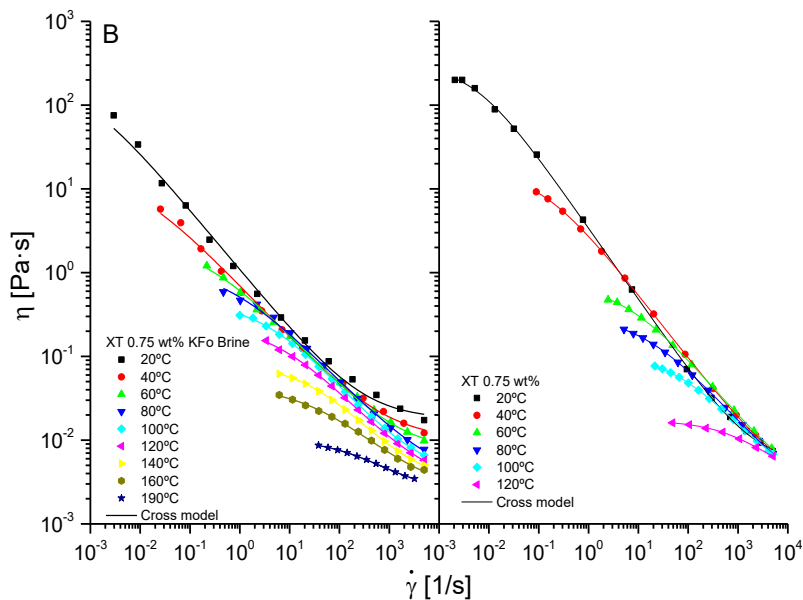
226 Figures 2A to 4A depict the flow curves of XT in formate brine, at selected  
 227 concentrations of XT, 0.25, 0.50 and 0.75 wt% respectively, in the range of temperature  
 228 from 20°C to 190°C. In Figures 2B to 4B the flow curves of the native XT solutions  
 229 have been included as reference.

230



231  
232  
233  
234

Figure 3. Evolution of the viscosity versus shear rate as a function of the temperature. A) Xanthan gum solution at 0.5wt% in potassium formate (KFo) brine. B) Xanthan gum solution at 0.5wt% in distilled water.



235  
236  
237  
238

Figure 4. Evolution of the viscosity versus shear rate as a function of the temperature. A) Xanthan gum solution at 0.75wt% in potassium formate (KFo) brine. B) Xanthan gum solution at 0.75wt% in distilled water.

239 Native XT solutions reveal their typical shear-thinning behavior, showing a trend for  
240 reach a zero-shear viscosity at lower shear rates, a pseudoplastic fall at intermediate  
241 shear-rate, and a slight tendency to reach an infinite shear viscosity in the high shear-  
242 rate region, beyond the experimental shear-rate window. As expected, the shear-  
243 thinning behavior of native XT solutions progressively vanishes as temperature  
244 increases approaching to the order-disorder transition. The side chains progressively  
245 lose their associations and the polymer is randomly dispersed in the solution, being less  
246 sensitive to shear (Pelletier et al., 2001). At temperatures above 120°C, the flow  
247 behavior is mainly Newtonian, independently of the XT concentration due to the  
248 thermal degradation of the ordered conformation of the biopolymer (Lambert and  
249 Rinaudo, 1985).

250 XT in formate brine retains the shear–thinning behavior over a wide range of  
251 temperature compared with the native solution. As can be seen in Figures 2A, 3A and  
252 4A, the pseudoplastic drop for XT in formate brine is slightly affected by the  
253 temperature until 140°C. Above this temperature, the solution becomes more sensitive  
254 to temperature, being more evident for solutions of lower XT content. The  
255 pseudoplastic region is shortened and a progressive decrease in the values of the shear  
256 viscosity, at a given shear rate, is observed as the temperature rises to 190°C.

257 To gain insight on the effect of temperature on the flow behavior of XT in formate brine  
258 solutions, Figure 5 shows the evolution of the zero-shear limiting viscosity and the  
259 infinite viscosity for XT in formate brine, estimated by the Cross' model as a function  
260 of temperature. The tendency on evolution of the zero-shear limiting viscosity for the  
261 native XT solutions has been also included for comparison.

262

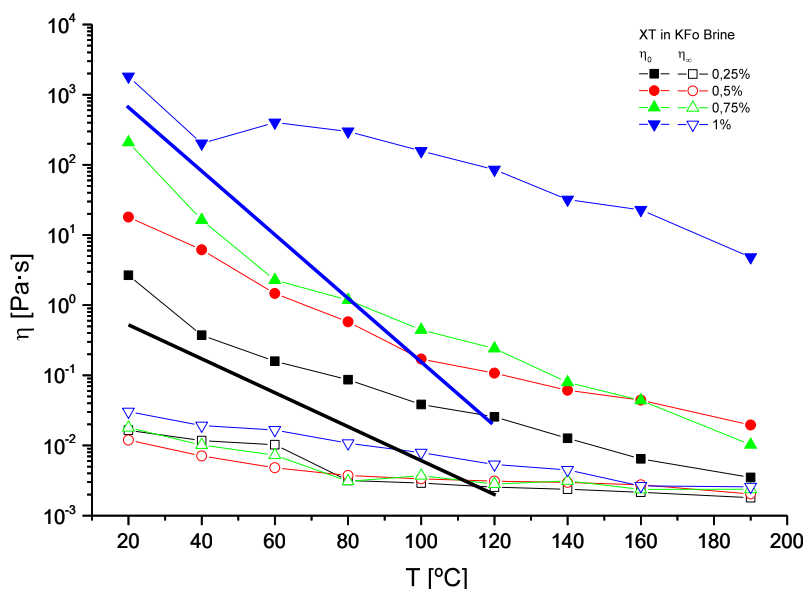


Figure 5. Evolution of the Cross's model, zero-shear-viscosity ( $\eta_0$ ) and infinite shear viscosity ( $\eta_\infty$ ) parameters, with the temperature for different concentrations of xanthan in KFo brine (lines and symbols). (Evolution of  $\eta_0$  for the native XT solutions, black line 0.25wt% and blue line 1.0wt%, included for comparison).

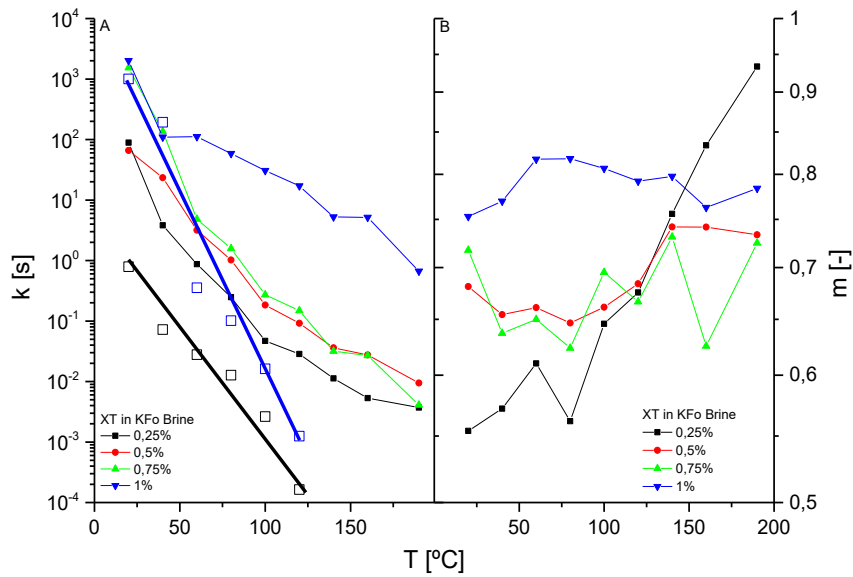
263  
264  
265  
266  
267

268 For native XT solutions at constant temperature, the zero-shear-limiting viscosity  
 269 increases exponentially with the concentration of XT, being 9.81C(wt%) at 20°C  
 270 decreasing for higher temperatures to 3.64C(wt%) at 100°C (results not shown in Figure  
 271 5). These results agree with those previously reported by other authors for XT solutions  
 272 without salt at similar concentration and temperature (Choppe et al., 2010; Wyatt et al.,  
 273 2009). At constant concentration, a higher negative slope in the evolution of the zero-  
 274 shear limiting viscosity with temperature is observed for the most concentrate native XT  
 275 solution (1 wt%, continuous line in Figure 5). The increase in thermal susceptibility  
 276 with XT concentration, in the range 20-120°C, would indicate the development of a  
 277 higher degree of weak association among polymer chains as the biopolymer content  
 278 increases (Choppe et al., 2010; Wyatt et al., 2009; Xie and Lecourtier, 1992).

279 XT solutions in formate brine exhibit a slightly lower exponential increasing of zero-  
 280 shear-limiting viscosity with concentration, nearly constant in the whole range of  
 281 temperature tested, around 8.5C(wt.%) (results not shown in Figure 6). The evolution of

282 zero-shear limiting viscosity with temperature is flattened and seems to be independent  
283 of XT concentration. Previous studies indicate that the evolution of the viscosity with  
284 temperature below the thermal transition can be modelled with both the Arrhenius  
285 model (Marcotte et al., 2001) and the WLF model (Pelletier et al., 2001), using shift  
286 factors based on the Time-Temperature Superposition Principle (TTSP). In this case,  
287 covering a larger temperature range, the decrease of the zero-shear limiting viscosity is  
288 less marked than those reported for less concentrated solutions (Choppe et al., 2010).  
289 This evolution can be modelled by empirical equations such as the Vogel model (result  
290 not shown). Consequently, formate brines, on the one hand, significantly decreases the  
291 thermal susceptibility of the XT solutions and, on the other hand, shifts the thermal  
292 transition to higher temperatures, as has been previously reported (Howard et al., 2015;  
293 Reinoso et al., 2019).

294 Figure 6 depicts the evolution of the parameters  $k$  and  $m$  of the Cross' model with  
295 temperature for the xanthan brine solutions studied. As expected, the time constant  $k$   
296 (Figure 6A) of the Cross' model is less sensitive to temperature for XT solutions in  
297 formate brine than for the native XT solutions, indicating the higher degree of  
298 structuring of the biopolymer. In addition, the power index (Figure 6B) remains  
299 approximately constant for XT concentration higher than 0.5 wt%. For the solution of  
300 0.25 wt%, a sharp increase of the power index is observed, indicating the sensitivity of  
301 this solution to thermal effects.

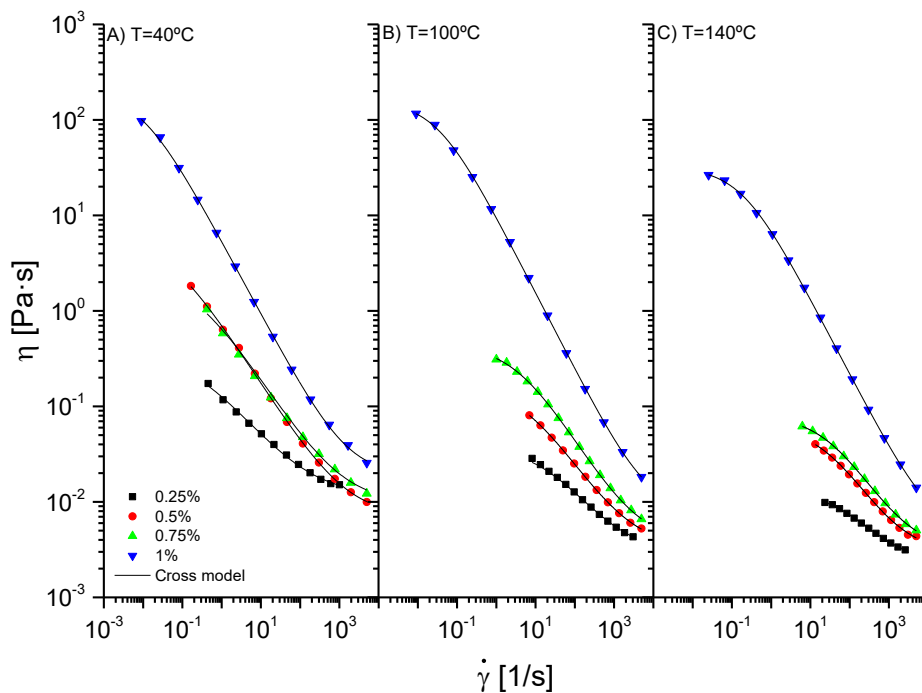


302  
 303  
 304  
 305  
 306  
 307  
 308

Figure 6. Evolution of the Cross's model time constant  $k$ , and the index  $m$ , with the temperature for different concentrations of xanthan in Kfo brine (line and symbols). (Evolution of parameter  $k$  for the native XT solutions, black line and open symbols 0.25wt% and blue line and open symbols 1.0wt%, included for comparison).

309  
 310

311 Figure 7 compares the flow curves, at selected temperatures, for XT solutions in  
 312 formate brine as function of XT concentration. It may be observed that both the shear-  
 313 thinning behavior and the viscosity values increase with XT concentration, being  
 314 practically non-susceptible to temperature. The enhancement of the thermal resistance  
 315 of XT in formate salts has been related to the capacity of the formate anion to reinforce  
 316 the structure of the biopolymer in solution by promoting hydrogen bonding and self-  
 317 association (Clarke-Sturman et al. 1986).

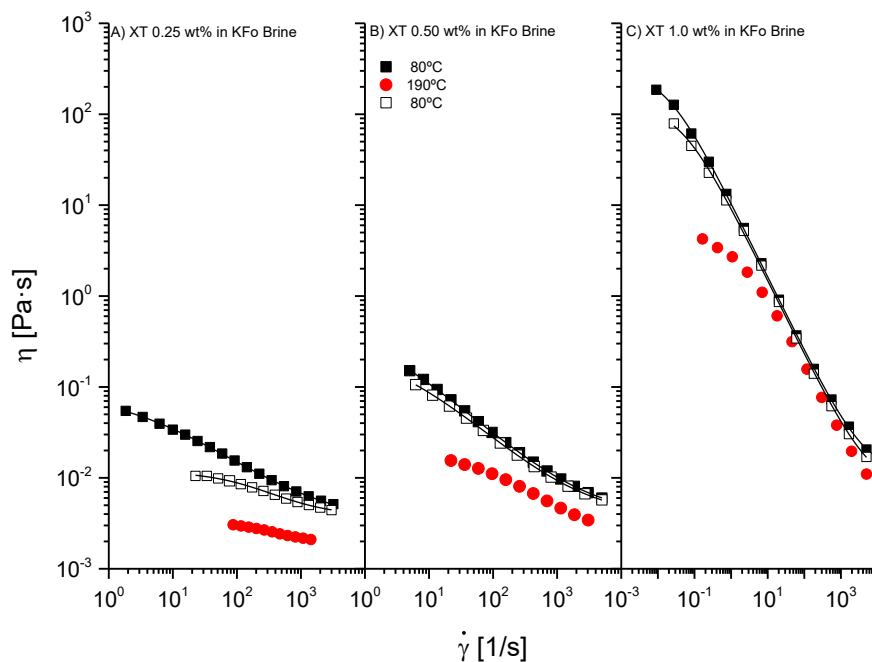


318

319 **Figure 7. Evolution of the viscosity versus shear rate as a function of xanthan concentration in potassium**  
 320 **formate brine (KFo). A) 40°C. B) 100°C. C) 140°C.**  
 321

322 Nevertheless, XT in solution experiences a slow degradation at high temperature as has  
 323 been reported in the literature (Howard et al., 2015; Lambert and Rinaudo, 1985). The  
 324 thermal degradation may decrease the recovery of the pseudoplasticity after exposing  
 325 the XT solutions to high temperature. In this sense, Figure 8 compares the flow curves  
 326 for selected XT concentrations in formate brine, measured at 80°C, before and after  
 327 submitting the sample to the stepwise program of temperatures for the flow  
 328 characterization from 80 to 190°C (steps at 80°C, 100°C, 120°C, 140°C, 160 °C, 190°C  
 329 and return to 80°C, 1.5 hours interval). In addition, the parameters of the Cross model  
 330 are presented in Table 1. As can be seen on Figure 8A, for low XT concentration (0.25  
 331 wt%) an important decrease in viscosity is observed over the whole region of shear rate  
 332 tested, more significantly in the low shear region. In contrast, the more concentrated XT  
 333 solutions recover the original pseudoplastic characteristic to a large extent after cooling

334 from 190°C to 80°C (see Fig. 8B and 8C for 0.5 and 1.0 wt%, respectively). These  
 335 results indicate that the effect of short-term thermal degradation on the pseudoplasticity  
 336 of XT solutions depends on XT concentration, being more significant for the low  
 337 concentrate solutions, where a lower degree of interactions between polymer chains  
 338 leads to a weaker gel structure, which exhibits a rheological behavior very sensitive to  
 339 polymer degradation. For the more concentrated XT solutions, a stronger structure  
 340 would be developed due to a higher degree of interactions between polymer chains  
 341 (higher density of chains), that damps the effect of thermal degradation on the bulk  
 342 viscosity of the solution. Nevertheless, high temperature destroys part of the structure,  
 343 as is indicated by the decrease in the values of zero-shear limiting viscosity, at 80°C,  
 344 displayed in Table 1 after submitting the solution to 190°C (62%, 53% and 45% of  
 345 decrease respectively). However, the power index  $m$  increases significantly only for  
 346 brine with low XT content (0.25 wt%), being practically the same for higher XT  
 347 concentration.



348

349 **Figure 8- Recovery of the pseudoplasticity, at 80°C, after submitting the sample at the temperature of 190°C.**

350 These results suggest that XT, at concentrations below 0.5 wt%, might have limited  
351 effectiveness as a component for rheology control in HP/HT environments where the  
352 drilling fluid is submitted at temperatures near 190°C due to the negative effect of the  
353 short-term degradation on the pseudoplasticity. An increase in XT concentration would  
354 mitigate these negative effects on the rheology, enlarging the time interval in which the  
355 fluid retains acceptable rheological properties for HP/HT applications.

356 The thermal degradation of pure XT starts around 232°C as has been reported by  
357 Srisvastava et al. from TGA results of pure polymer (Srivastava et al., 2012). In  
358 solution, the thermal stability of XT increases in the presence of salts (Lambert et al.,  
359 1985; Xie and Lecourtier, 1992) where the ionic strength would protect the helical  
360 structure from the chemical attack. Several mechanisms of degradation of the structure  
361 and properties of XT in solution such as mechanical degradation, free-radicals,  
362 hydrolysis and enzymatic degradation have been proposed in the literature (Ash et al.,  
363 1983; Wellington, 1983).

364 The XT solutions in formate brine studied in this work show high resistance to  
365 mechanical degradation when they were submitted to shear loops in the range  $10^3$ - $5 \cdot 10^3$   
366  $s^{-1}$  even at the highest temperature of 190°C, in agreement with the good mechanical  
367 resistance reported previously for XT solutions of similar concentration submitted to the  
368 shear conditions typical in oilfield (Seright et al., 2011).

369 Free-radicals oxidation of the hydroxyl groups has been proposed as a degradation  
370 mechanism for XT solutions in the presence of oxygen. Oxidation can be minimized  
371 reducing the oxygen concentration in solution via oxygen scavengers and increasing the  
372 brine concentration (Wellington, 1983). In this sense, the thermal resistance of XT  
373 solution in formate brines has been related to a slowdown of the degradation of the  
374 structure due to the antioxidant properties of the formate anion in combination with the

375 salting out of the presence of the cations (Howard et al., 2015). For these XT solutions,  
 376 a minimal concentration of oxygen could remain in the pressure cell even though it was  
 377 pressurized with 50 bar of Nitrogen, thus some degree of oxidative degradation would  
 378 be possible.

379  
 380  
 381

**Table 1. Parameters of the Cross' model for different concentration of XT in formate brine, samples were submitted to temperatures of 80°C-190°C-80°C at 50 bar of pressure.**

XT 0.25 wt% in KFo brine			
	80°C	190°C	80°C
$\eta_0$ (Pa·s)	0,0864	0,0035	0,0122
$\eta_\infty$ (Pa·s)	0,0031	0,0018	0,0038
k (s)	0,247	0,0034	0,0055
m (-)	0,562	0,933	0,871
XT 0.5 wt% in KFo brine			
	80°C	190°C	80°C
$\eta_0$ (Pa·s)	0,5789	0,0196	0,2726
$\eta_\infty$ (Pa·s)	0,0037	0,0020	0,0037
k (s)	1,020	0,0094	0,342
m (-)	0,646	0,734	0,658
XT 1.0 wt% in KFo brine			
	80°C	190°C	80°C
$\eta_0$ (Pa·s)	299,2	4,825	124,813
$\eta_\infty$ (Pa·s)	0,0107	0,0025	0,0076
k (s)	58,64	0,667	22,62
m (-)	0,818	0,784	0,818

382  
 383 Other mechanisms such as the hydrolysis of acetyl groups have also been suggested as  
 384 responsible of short-term XT degradation at high temperature (Seright and Henrici,  
 385 1990; Wellington, 1983). For these solutions, the initial pH measured in the solution, at  
 386 80°C, before pressurizing was around 8.1 and the final value, after submitting the  
 387 sample to 190°C, returning to 80°C, and depressurizing was around 7.5. In this range of  
 388 pH, XT solutions in brines show maximum thermal stability against hydrolysis as has  
 389 been reported by Seright and Henrici (1990), therefore, degradation by hydrolysis seems  
 390 to be unlikely. Further systematic studies would be necessary to understand the nature  
 391 and kinetic of XT degradation at high temperature in concentrated formate brines, this

392 would then provide a basis to improve the development of fluids for HP/HT  
393 applications.

#### 394 **4. Conclusions**

395 Xanthan solutions at moderate concentration in potassium and calcium concentrated  
396 brines show non-Newtonian pseudoplastic behavior that can be modelled by the Cross'  
397 model in the range of temperature of 20-190°C. Potassium brines shift the reversible  
398 thermal conformational transition of XT to higher temperatures, retaining the non-  
399 Newtonian properties over a wide range of temperatures, mainly formate brine.

400 XT in formate brine experiences a slow thermal degradation process at high temperature  
401 that decreases the recovery of the pseudoplasticity after exposing the solutions to high  
402 temperature. The detrimental effect of short-term thermal degradation is characterized  
403 by a decrease in the values of both the zero-shear limiting viscosity, the time constant  $k$ ,  
404 and an increase in the value of the index,  $m$ , being more significant for low polymer  
405 concentration. An increase in XT concentration, would mitigate these negative effects  
406 on the rheology, enlarging the time interval in which the fluid retains acceptable  
407 rheological properties for HP/HT applications.

408 From the structural point of view, the low density of chains in low concentrate XT  
409 solutions would lead to the development of weaker gel structures, with rheological  
410 behavior very sensitive to thermal degradation of the side chains, probably due to  
411 irreversible free-radical oxidations at high temperature. The increase of XT  
412 concentration enhances the strength of the structure, softening the effect of the thermal  
413 degradation on the pseudoplastic behavior.

414 **Acknowledgements**

415 This work was supported by the Spanish Ministry of Economy, Industry and  
416 Competitiveness (Project CTQ2017-89792-R (AEI/FEDER, EU)) and the Spanish  
417 Ministry of Economy and Competitiveness (Project CTQ2014-56980-R  
418 (MINECO/FEDER)).

419        **5. References**

- 420 Asafa, K. A., Shah, S. N. Rheology and Flow Characteristics of Xanthan in Calcium  
421 Chloride Brine. Society of Petroleum Engineers. (2014, March 25).  
422 doi:10.2118/168289-MS
- 423 Ash, S.G., Clarke-Sturman, A. J., Calvert, R., Nisbet, T. M. Chemical Stability of  
424 Biopolymer Solutions, SPE (1983). doi:10.2118/12085-MS
- 425 Bergmann, D., Furth, G., Mayer, C. Binding of bivalent cations by xanthan in aqueous  
426 solution, *Int. J. Biol. Macromol.* 43 (2008) 245–251.  
427 doi:10.1016/j.ijbiomac.2008.06.001
- 428 Boul, P.J., Abdulquddos, S., Thaemlitz, C.J. High Performance Brine Viscosifiers for  
429 High Temperatures, SPE, 2017. <https://doi.org/10.2118/183964-MS>
- 430 Bradshaw, R. J., Hodge, R. M., Wolf, N. O., Knox, D. A., Hudson, C. E., Evans, E.  
431 Formate-Based Reservoir Drilling Fluid Resolves High-Temperature Challenges in the  
432 Natuna Sea. Society of Petroleum Engineers. (2006, January 1). doi:10.2118/98347-MS
- 433 Caenn, R., Darley, H.C.H., Gray, G.R. Composition and Properties of Drilling Fluids  
434 and Completion Fluids, seventh ed., Gulf Professional Publishing, Houston, 2017.
- 435 Choppe, E., Puaud, F., Nicolai, T., Benyahia, L. Rheology of xanthan solutions as a  
436 function of temperature, concentration and ionic strength, *Carbohydr. Polym.* 82(4)  
437 (2010) 1228–1235. doi:10.1016/j.carbpol.2010.06.056
- 438 Clarke-Sturman, A.J., Pedley, J.B., Sturla, P.L. Influence of anions on the properties of  
439 microbial polysaccharides in solution, *Int. J. Biol. Macromol.* 8 (1986) 355-360.
- 440 Cross, M.M. Rheology of non-Newtonian fluids: A new flow equation for pseudoplastic  
441 systems, *J. Colloid Sci.* 20 (1965) 417-434.
- 442 Dario, A.F., Hortencio, L.M.A., Sierakowski, M.R., Queiroz Neto, J.C., Petri, D.F.S.  
443 The effect of calcium salts on the viscosity and adsorption behavior of xanthan,  
444 *Carbohydr. Polym.* 84 (2011) 669–676. doi:10.1016/j.carbpol.2010.12.047
- 445 Fitzpatrick, P., Meadows, J., Ratcliffe, I., Williams, P.A. Control of the properties of  
446 xanthan/glucomannan mixed gels by varying xanthan fine structure, *Carbohydr. Polym.*  
447 92 (2013) 1018–1025. <http://dx.doi.org/10.1016/j.carbpol.2012.10.049>

448 Gao, C. H. (2019, June 1). A Survey of Field Experiences With Formate Drilling Fluid.  
449 Society of Petroleum Engineers. doi:10.2118/195699-PA

450 Garcia-Ochoa, F., Santos, V.E., Casas, J.A., Gomez, E. Xanthan gum: Production,  
451 recovery, and properties, *Biotechnol. Adv.* 18 (2000) 549–579.

452 Ghoumrassi-Barr, S., Aliouche, D.A. Rheological Study of Xanthan Polymer for  
453 Enhanced Oil Recovery, *J. Macromol. Sci. Part B Phys.* 55, 8 (2016) 793–809.  
454 <https://doi.org/10.1080/00222348.2016.1207544>

455 Hermoso, J. Martinez-Boza, F. Gallegos, C. Influence of aqueous phase volume  
456 fraction, organoclay concentration and pressure on invert-emulsion oil muds rheology.  
457 *J. Ind. Eng. Chem.* 22 (2015) 341–349. <https://doi.org/10.1016/j.jiec.2014.07.028>

458 Hermoso, J. Martínez-Boza, F. J. Gallegos, C. Organoclay influence on high pressure-  
459 high temperature volumetric properties of oil-based drilling fluids. *J. Petrol. Sci. Eng.*  
460 151 (2017) 13-23. <https://doi.org/10.1016/j.petrol.2017.01.040>

461 Howard, S., Kaminski, L., Downs, J. Xanthan stability in formate brines - Formulating  
462 non-damaging fluids for high temperature applications, SPE European Formation  
463 Damage Conference and Exhibition 2015, 116921S (2015) 1388-1413.  
464 doi:10.2118/174228-MS

465 Jang, H.Y., Zhang, K., Chon, B.H., Choi, H.J. Enhanced oil recovery performance and  
466 viscosity characteristics of polysaccharide xanthan gum solution, *J. Ind. Eng. Chem.* 21  
467 (2015) 741–5. <https://doi.org/10.1016/j.jiec.2014.04.005>

468 Lambert, F. Rinaudo, M. On the thermal stability of xanthan. *Polymer* 26, (1985) 1549-  
469 1553.

470 Lambert, F., Milas, M., Rinaudo, M. Sodium and calcium counterion activity in the  
471 presence of xanthan polysaccharide, *Int. J. Biol. Macromol.* 7 (1985) 49-52.

472 Marcotte, M., Taherian, A.R., Hoshahili, H.S. Ramaswamy, Rheological properties of  
473 selected hydrocolloids as a function of concentration and temperature, *Food Res. Int.*  
474 34(8) (2001) 695–703.

475 Mezger, T. G. *The Rheology Handbook*, 4th Edition. Vincentz Network, Hanover, 2014

476 Nieto Galván, Z.R. Soares, L.S., Medeiros, A.E.A., Soares, N.F.F., Ramos, A.M.,  
477 Coimbra, J.S.R., Oliveira, E.B. Rheological properties of aqueous dispersions of

478 xanthan gum containing different chloride salts are impacted by both sizes and net  
479 electric charges of the cations, *Food Biophys.* 13 (2018) 186–197.  
480 <https://doi.org/10.1007/s11483-018-9524-9>

481 Pelletier, E., Viebke, C., Meadows, J., Williams, P.A. A Rheological Study of the  
482 Order–Disorder Conformational Transition of Xanthan Gum, *Biopolym.* 59 (2001) 339–  
483 346.

484 Reinoso, D., Martin-Alfonso, M.J., Luckham, P.F., Martinez-Boza, F.J. Rheological  
485 characterisation of xanthan gum in brine solutions at high temperature. *Carbohydr.*  
486 *Polym.* (2019), 203, 103–109. <https://doi.org/10.1016/j.carbpol.2018.09.034>

487 Rochefort, W.E., Middleman, S. Rheology of xanthan gum: Salt, temperature, and strain  
488 effects in oscillatory and steady shear experiments, *J. Rheol.* 31(4) (1987) 337–369.  
489 <https://doi.org/10.1122/1.549953>

490 Ross-Murphy, S.B. Structure-property relationships in food biopolymer gels and  
491 solutions. *J. Rheol.* 39(6) (1995) 1451-1463. <https://doi.org/10.1122/1.550610>

492 Seright, R. S., Fan, T. Wavrik, K. Balaban, R. C. New Insights Into Polymer Rheology  
493 in Porous Media. *SPE J.* 16(1), (2011) 35-42. doi:10.2118/129200-PA

494 Seright, R.S., Henrici, B.J. Xanthan Stability at Elevated Temperatures, *SPE Reservoir*  
495 *Eng.*, 5(1) (1990) 52-60. <https://doi.org/10.2118/14946-PA>

496 Song, K.W., Kim, Y.S., Chang, G.S. Rheology of concentrated xanthan gum solutions:  
497 Steady shear flow behaviour, *Fibers Polym.* 7(2) (2006) 129–138.  
498 <https://doi.org/10.1007/BF02908257>

499 Srivastava, A., Mishra, V., Singh, P., Srivastava, A., Kumar, R. Comparative study of  
500 thermal degradation behavior of graft copolymers of polysaccharides and vinyl  
501 monomers, *J. Therm. Anal. Calorim.* 107 (2012) 211–223.  
502 <https://doi.org/10.1007/s10973-011-1921-y>

503 Sutherland, AN.W. Structure-function relationships in microbial exopolysaccharides,  
504 *Biotechnol. Adv.* 12 (1994) 393-448.

505 Wei, B., Romero-Zerón, L., Rodrigue D., Mechanical properties and flow behavior of  
506 polymers for enhanced oil recovery, *J. Macromol. Sci. Part B Phys.* 53 (4) (2014) 625-  
507 644. <http://dx.doi.org/10.1080/00222348.2013.857546>

508 Wellington, S. L. Biopolymer Solution Viscosity Stabilization - Polymer Degradation  
509 and Antioxidant Use, SPE J. 23(6) (1983) 901-912. doi:10.2118/9296-PA.

510 Whitcomb, P.J., Macosko, C.W. Rheology of xanthan gum, J. Rheol. 22(5) (1978) 493–  
511 505. <https://doi.org/10.1122/1.549485>

512 Wyatt, N.B., Gunther, C.M., Liberatore, M.W. Increasing viscosity in entangled  
513 polyelectrolyte solutions by the addition of salt, Polymer 52 (11) (2011) 2437-2444.  
514 doi:10.1016/j.polymer.2011.03.053

515 Wyatt, N.B., Liberatore, M.W. Rheology and viscosity scaling of the polyelectrolyte  
516 xanthan gum, J. Appl. Polym. Sci. 114(6) (2009) 4076–4084. DOI 10.1002/app.31093

517 Xie, W., Lecourtier, J. Xanthan behaviour in water-based drilling fluids, Polym.  
518 Degrad. Stab., 38 (1992) 155–164.